An investigation of two-dimensional parameter-induced stochastic resonance and applications in nonlinear image processing

2009 J. Phys. A: Math. Theor. 42 145207

(http://iopscience.iop.org/1751-8121/42/14/145207)

J. Phys. A: Math. Theor. **42** (2009) 145207 (9pp) doi:10.1088/1751-8113/42/14/145207

An investigation of two-dimensional parameter-induced stochastic resonance and applications in nonlinear image processing

Yibing Yang[1], Zhongping Jiang[2], Bohou Xu[1] and Daniel W Repperger[3]

[1] Department of Mechanics, State Key Laboratory of Fluid Power Transmission and Control, Zhejiang University, Hangzhou 310027, People's Republic of China
[2] Department of Electrical and Computer Engineering, Polytechnic Institute of NYU, Brooklyn, NY 11201, USA
[3] Air Force Research Laboratory, Wright-Patterson AFB, OH 45433, USA

E-mail: xubohou@zju.edu.cn

Received 4 December 2008, in final form 19 February 2009
Published 17 March 2009
Online at stacks.iop.org/JPhysA/42/145207

Abstract
This paper aims at developing an elementary theory of two-dimensional (2D) parameter-induced stochastic resonance (PSR) to contribute to nonlinear image processing. In order to tackle the application of SR in image processing, where adding noise may not be an easy task, we propose to generalize the concept of PSR from the one-dimensional (1D) case to the 2D case. An interesting feature of this paper is that a rigorous analytical framework is developed based on the Fokker–Planck equation (FPE). Some applications to image processing are performed to demonstrate the effectiveness of the approaches based on the proposed theory of 2D PSR. It is believed that the PSR-based methodology as advocated in this paper provides a different, but promising perspective for applying SR techniques to nonlinear image processing.

PACS numbers: 05.40.−a, 02.50.−r

1. Introduction

In order to introduce the mechanism of stochastic resonance (SR), let us consider a heavily damped particle of mass m and viscous friction γ, moving in a symmetric double-well potential $U(x)$ (see figure 1(a)). If we apply a weak periodic forcing to the particle, the double-well potential would be tilted asymmetrically up and down, periodically raising and lowering the potential barrier, as shown in figure 1(b). The fluctuational forces cause transitions between the neighboring potential wells with a rate named Kramers rate [1]. Generally, the weak periodic forcing itself cannot cause the particle to roll periodically from one potential well into the other one. However, noise-induced hopping between the potential wells can become

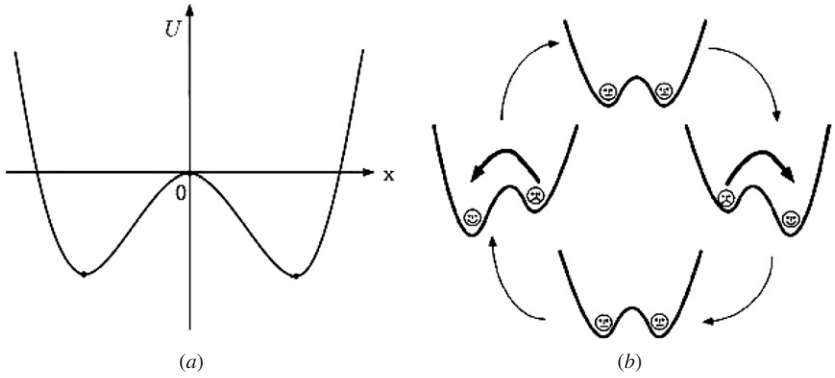

Figure 1. (*a*) Symmetric double-well potential. (*b*) Double-well potential under periodic weak forcing.

synchronized with the weak periodic forcing. This statistical synchronization takes place when the average waiting time between two noise-induced inter-well transitions is comparable with half the period of the periodic forcing. This phenomenon is called stochastic resonance.

Usually, noise is thought to be annoying. Stochastic resonance, in contrast, is a phenomenon in which noise can be used to enhance, rather than hinder, the system performance. For example, the output signal-to-noise ratio (SNR) of the double-well SR system will be maximized when an optimal amount of additional noise is added to the input [1]. The concept of SR was first proposed by Benzi in 1981, addressing the problem of the periodically recurrent ice ages [2]. It has a broad range of application areas, such as in physics, chemistry, biomedical sciences and engineering systems [1, 3–7]. Balance control and speech understanding are just two of its applications. The balance control abilities of elderly people can be enhanced with the aid of noise [3]. Profoundly deaf people can better understand speech when a certain amount of noise is added to the vowel coding for cochlear implants [3]. Other applications include signal detection [5, 8–13], signal transmission [6, 14] and signal estimation [7].

The noise can become beneficial, but only when the synchronization between the input signal and the noise occurs through a properly chosen nonlinear system. For conventional SR, the SR effect is realized by adding an optimal amount of noise into the system [1]. Recently, a new approach, called parameter-induced stochastic resonance (PSR), is proposed to realize the synchronization by optimally tuning the system parameters without adding any noise [15–21]. It has been proved that by adjusting the parameters, SR realized by the conventional method (adding noise) is an optimization problem in a subregion of the parameter space [15]. When SR is realized by tuning the system parameters (with some fixed noise level) at an inner point of the parameter space, the fixed noise level is just the optimum noise level for the conventional SR. We have already successfully applied PSR to one-dimensional (1D) signal processing, such as the recovery of noisy multi-frequency signals [16] and the transmission of baseband binary signals over noisy channels [19].

In fact, besides 1D signal processing applications, image processing is another potential application area of SR techniques. Image processing techniques have been widely applied to different areas, such as diagnosing tumors in medical images, detecting and identifying hostile targets in military images. In order to enhance the images corrupted by noise, de-noising algorithms are conventionally used to remove or suppress noise from the images. Recently,

some research results taking advantage of noise have been obtained on image processing using the SR technique [22–25]. However, two main shortcomings may be identified. First, most of these research papers are based on simulations and lack theoretical analysis. Second, these approaches are based on the conventional SR method by adding an optimal additional noise into the system, which is not practical for some image processing applications. In contrast, PSR can achieve the SR effect without adding any noise. But our initial research has shown that it is not effective to directly process the images using 1D bistable filters because every image pixel is related to pixels nearby in any direction. In order to extend the applications of SR techniques in the image processing area, an entirely new theory about 2D SR must be developed. This paper aims at developing a theoretical foundation of 2D PSR for the application of SR in image processing without adding any noise. A new 2D nonlinear SR system is first proposed by extending the concept of PSR from the 1D case to the 2D case. The stochastic characteristics of this SR system are then derived. It is our belief that the approach based on our proposed 2D PSR provides an innovative and promising method to nonlinear image processing using SR techniques.

2. Two-dimensional SR systems and the related Fokker–Planck equation

Similar to the one-dimensional nonlinear bistable SR system [15], we propose the following two-dimensional nonlinear SR system:

$$\frac{\partial^2 w}{\partial x \partial y} = -\gamma \left(\frac{\partial w}{\partial x} + \frac{\partial w}{\partial y} \right) + f(w) + \Gamma(x, y), \tag{1}$$

where $w = w(x, y)$ is the state variable (system output), $\gamma\left(\frac{\partial w}{\partial x} + \frac{\partial w}{\partial y}\right)$, $(\gamma > 0)$ is the damping term, $f(w) = -\frac{\partial U(w)}{\partial w} = aw - bw^3 + h$, $U(w)$ is the double-well potential, h is the original signal, γ, a, b are the system parameters to be adjusted, and $\Gamma(x, y)$ is the Gaussian white noise with

$$\langle \Gamma(x, y)\Gamma(x_1, y_1) \rangle = 2D\delta(x - x_1, y - y_1). \tag{2}$$

Here D is the noise intensity, and is related to noise variance σ^2 by $\sigma^2 = \frac{D}{\Delta t^2}$ in the 2D case, where Δt is the sampling interval in both directions x and y. $h + \Gamma(x, y)$ can be viewed as the input.

First, we reduce the partial differential equation (1) to a set of ordinary differential equations along the line $x = x_0 + t\Delta x$, $y = y_0 + t\Delta y$ (here Δx, Δy represent the lengths of one pixel. For convenience, we define $\Delta x = \Delta y = 1$). Equation (1) then becomes

$$\begin{cases} \dfrac{\mathrm{d}w}{\mathrm{d}t} = \Delta x v = v, \\ \dfrac{\mathrm{d}v}{\mathrm{d}t} = -\gamma(\Delta x + \Delta y)v + \Delta y f(w) + \dfrac{1}{\Delta x}\Gamma_1(t) \ = -2\gamma \cdot v + f(w) + \Gamma_1(t), \end{cases} \tag{3}$$

where $\langle \Gamma_1(t)\Gamma_1(t_1) \rangle = 2D\delta(t - t_1)$. The corresponding Fokker–Planck equation (FPE) [26] for probability density function (PDF) $\rho(w, v, t)$ is

$$\frac{\partial \rho(w, v, t)}{\partial t} = -\frac{\partial}{\partial w}[v\rho(w, v, t)] - \frac{\partial}{\partial v}[(-2\gamma \cdot v + f(w))\rho(w, v, t)] + D\frac{\partial^2 \rho(w, v, t)}{\partial v^2}. \tag{4}$$

Note that equation (4) is clearly independent of (x_0, y_0), thus the solution of this equation will be valid for any (x_0, y_0).

2.1. Stationary solution of equation (4)

Let $\rho_0(w, v)$ be the stationary solution satisfying the following equation:

$$-\frac{\partial}{\partial w}[v\rho_0(w, v)] - \frac{\partial}{\partial v}[(-2\gamma \cdot v + f(w))\rho_0(w, v)] + D\frac{\partial^2 \rho(w, v, t)}{\partial v^2} = 0. \tag{5}$$

The solution of equation (5) is

$$\rho_0(w, v) = \mathrm{e}^{-\phi(w,v)}, \tag{6}$$

where

$$\phi(w, v) = \frac{\gamma}{D}v^2 - \frac{2\gamma}{D}\int_0^w f(w)\,\mathrm{d}w - \ln N_0, \tag{7}$$

with N_0 being the normalized factor.

2.2. Non-stationary solution of equation (4)

We rewrite equation (4) as

$$\frac{\partial \rho}{\partial t} = -\frac{\partial}{\partial w}(D_1\rho) - \frac{\partial}{\partial v}(D_2\rho) + D_{22}\frac{\partial^2 \rho}{\partial v^2} = L_{\mathrm{FP}}(\rho), \tag{8}$$

where $L_{\mathrm{FP}}(\bullet)$ is the Fokker–Planck operator and

$$D_1 = v, \qquad D_2 = -2\gamma \cdot v + f(w), \qquad D_{22} = D. \tag{9}$$

Letting $\rho = \xi(w, v)\,\mathrm{e}^{-\lambda t}$, equation (8) becomes

$$\lambda\xi(w, v) = -L_{\mathrm{FP}}\xi(w, v). \tag{10}$$

This is an eigenvalue problem of the operator $-L_{\mathrm{FP}}(\bullet)$. Thus the solution of equation (8) can be written as [15]

$$\rho(w, v, t) = \rho_0(w, v) + \rho_1(w, v)\,\mathrm{e}^{-\lambda_1 t} + \rho_2(w, v)\,\mathrm{e}^{-\lambda_2 t} + \cdots, \tag{11}$$

where $\rho_0(w, v)$ is the stationary solution, $\rho_1(w, v)$, $\rho_2(w, v)$, ..., are determined by the initial conditions, $\lambda_1, \lambda_2, \ldots$, are the eigenvalues of $-L_{\mathrm{FP}}(\bullet)$.

Assuming $\mathrm{Re}\,\lambda_1 < \mathrm{Re}\,\lambda_2 < \cdots$, the term $\rho_1(w, v)\,\mathrm{e}^{-\lambda_1 t}$ of equation (11) will dominate the transient process. We define $\mathrm{Re}\,\lambda_1$ as the response speed of the system (4). Let

$$\xi(w, v) = \psi(w, v)\,\mathrm{e}^{-\phi/2}, \tag{12}$$

where ϕ is defined in (7). Thus, equation (10) becomes

$$\lambda\psi = -L\psi, \tag{13}$$

where L is a differential operator defined by

$$\begin{aligned} L\psi &= \mathrm{e}^{\phi/2}L_{\mathrm{FP}}(\mathrm{e}^{-\phi/2}\psi) \\ &= \mathrm{e}^{\phi/2}\frac{\partial}{\partial w}(D_1\,\mathrm{e}^{-\phi/2}\psi) - \mathrm{e}^{\phi/2}\frac{\partial}{\partial v}(D_2\,\mathrm{e}^{-\phi/2}\psi) + \mathrm{e}^{\phi/2}D_{22}\frac{\partial^2}{\partial v^2}(\mathrm{e}^{-\phi/2}\psi). \end{aligned} \tag{14}$$

Furthermore, we assume that ψ has the following asymptotic property:

$$\psi(w, v) = O(\mathrm{e}^{-\phi/2}), \qquad w \to \pm\infty, \qquad v \to \pm\infty. \tag{15}$$

As calculating λ_1 is quite complicated, we will then calculate, instead, the eigenvalues of the symmetric part $-L_s$ of the operator $-L_{\mathrm{FP}}(\bullet)$:

$$L_s = \frac{1}{2}(L + L^c) = \mathrm{e}^{\phi/2}\frac{\partial}{\partial v}\left[D_{22}\,\mathrm{e}^{-\phi}\frac{\partial}{\partial v}(\mathrm{e}^{\phi/2})\right]. \tag{16}$$

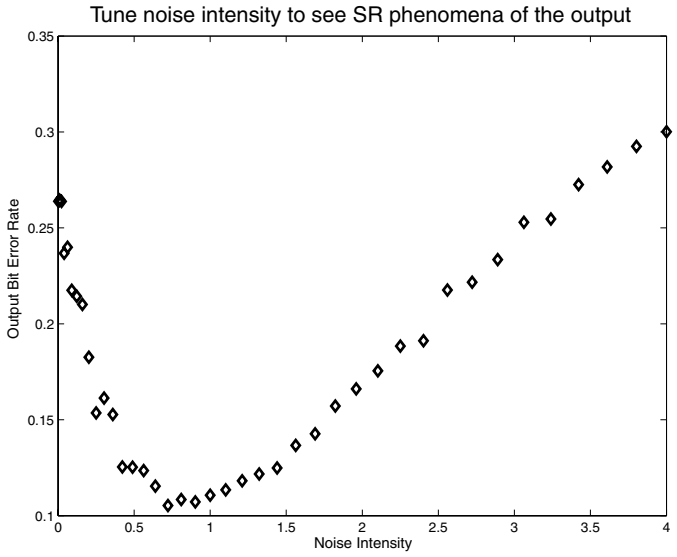

Figure 2. In simulation, we tune noise intensity from zero to 4 to see the SR phenomenon of the output image. The system parameters are $\gamma = 0.1, a = 0.5, b = 0.01$.

It is obvious that $-L_s$ is a semi-positive definite operator. Therefore, the eigenvalues of $-L_s$ as $\lambda_0^s, \lambda_1^s, \lambda_2^s, \ldots$, are real and nonnegative. Assuming $0 = \lambda_0^s < \lambda_1^s \leqslant \lambda_2^s \leqslant \cdots$, we have proved that λ_1^s is a lower bound of $\mathrm{Re}\,\lambda_1$. In the following sections, we regard λ_1^s as the response speed to estimate the speed tending to the stationary solution. When $\lambda_1^s t >> 1, \rho(w, v, t) \approx \rho_0(w, v)$. In practice, we often choose $\lambda_1^s t = 3$. Thus the error magnitude is about $e^{-3} \approx 0.05$ which can be acceptable. λ_j^s can be written as the Rayleigh quotient form:

$$\lambda_j^s = \underset{\psi \neq 0}{\text{st.}} \frac{\iint D_{22} \cdot \mathrm{e}^{-\phi}\left[\frac{\partial}{\partial v}(\mathrm{e}^{\phi/2}\psi)\right]^2 \mathrm{d}w\,\mathrm{d}v}{\iint \psi^2\,\mathrm{d}w\,\mathrm{d}v}, \qquad j = 0, 1, 2, \ldots, \tag{17}$$

where st.(•) is the stationary value of the functional.

3. Image processing using 2D PSR

Suppose a binary image (image with two gray degrees, $h = +A$ for white and $h = -A$ for black) is corrupted by a Gaussian white noise. The 2D bistable system (1) can be used as a nonlinear filter to process noisy images and improve its quality, and its output bit error rate (BER) can be written as [19]

$$P_e \approx P_A \int_{-\infty}^{0} \rho(w, T_b\,|A)\,\mathrm{d}w + P_{-A} \int_{0}^{+\infty} \rho(w, T_b\,|-A)\,\mathrm{d}w, \tag{18}$$

where $\rho(w, T_b|\pm A) = \int_{-\infty}^{+\infty} \rho(w, v, T_b)\,|_{h=\pm A}\,\mathrm{d}v$, $\rho(w, v, Tb)$ is obtained from equation (11) where the first two terms are retained, T_b is the length of pixels with the same input value h, P_A and P_{-A} are the probabilities of the input value being $+A$ or $-A$. Thus the optimization problem is described as

$$\min_{\gamma,a,b;\, D=\text{const},\lambda_1^s T_b \approx 3} P_e. \tag{19}$$

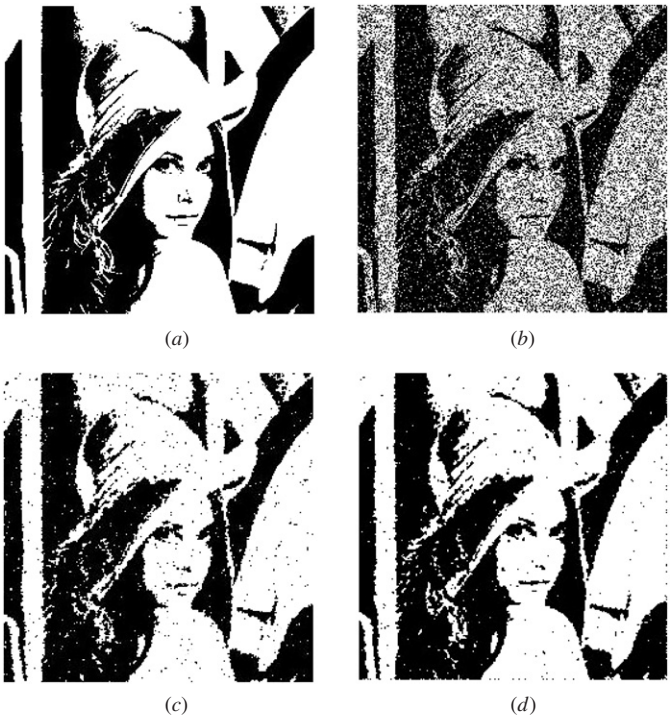

Figure 3. (*a*) Original image. (*b*) Image corrupted by Gaussian white noise with $D = 1$. (*c*) De-noise image using equation (20) with $\gamma = 0.775$, $a = -0.75$, $b = 0.2$ and BER $= 6.92\%$. (*d*) De-noise image using low-pass spacial filter with impulse response

$$h = \frac{1}{9}\begin{bmatrix} 1 & 1 & 1 \\ 1 & 1 & 1 \\ 1 & 1 & 1 \end{bmatrix}$$

and zero threshold, the output BER $= 8.08\%$.

In dealing with equation (19) we first choose $\lambda_1^s T_b = 3$ to make the error magnitude less than 0.05. Thus the equation has only two parameters independent, which can be solved by the recursion algorithm [17, 27].

When the parameters of the system are chosen, we can easily implement equation (1) by the difference method [28]:

$$\begin{aligned} w(m,n) = {} & (1+\gamma\cdot\Delta t)\cdot[w(m,n-1)+w(m-1,n)] \\ & -(1-2\gamma\cdot\Delta t)\cdot w(m-1,n-1)+x(m-1,n-1)\cdot\Delta t^2 \\ & +[a\cdot w(m-1,n-1)-b\cdot w(m-1,n-1)^3]\cdot\Delta t^2, \end{aligned} \tag{20}$$

where $x = h + \Gamma$ is the input, Δt is step length, for example, if the sampling frequency is 100 per pixel (ten by row and ten by column), $\Delta t = 0.1$. The boundary condition is often set to be zero. Here γ, a, b are the optimized parameters by equation (19).

Calculating λ_1^s requires two double integrations. Calculating Pe also requires two double integrations. How complex the optimization is depends on the number of recursions. Fortunately, the recursion would converge in a few steps [17]. After optimizing parameters, it is then quite efficient to process an image with equation (20), for it is a recursive difference equation.

In order to see the phenomenon of traditional SR (that is, output performance reaches a peak when increasing input noise), we use equation (20) with fixed system parameter γ, a, b to process a noise-corrupted image where the input noise intensity is tunable. Figure 2 depicts

(*a*) (*b*) (*c*)

Figure 4. (*a*) Image corrupted by Gaussian white noise with $D = 4$. (*b*) De-noise image using equation (20) with $\gamma = 0.8, a = -0.025, b = 0.05$ and BER $= 11.58\%$. (*c*) De-noise image using a low-pass spacial filter, the output BER $= 14.20\%$.

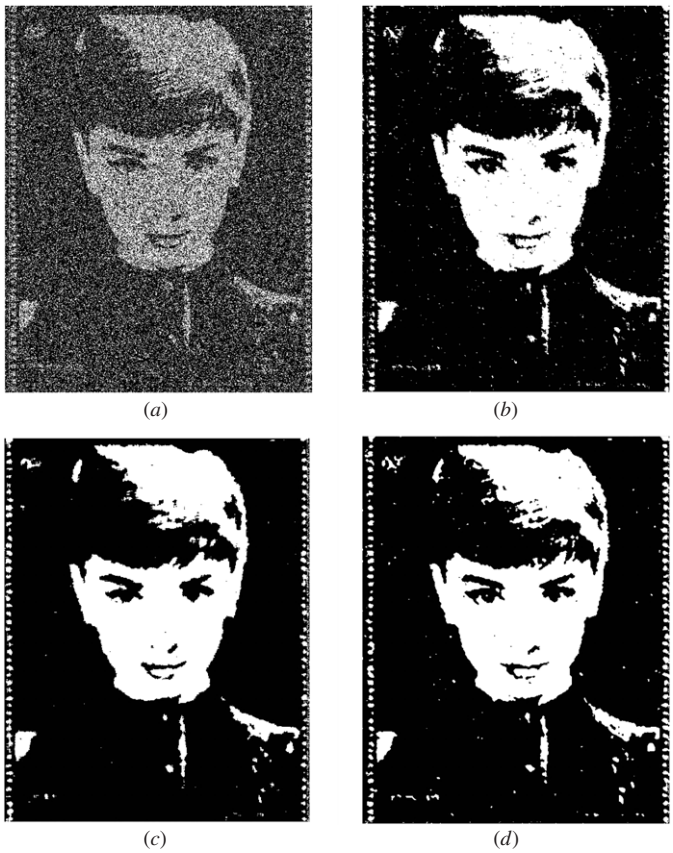

(*a*) (*b*)

(*c*) (*d*)

Figure 5. (*a*) Image corrupted by Gaussian white noise with $D = 4$. (*b*) De-noise image using equation (20) with $\gamma = 0.725, a = -0.1, b = 0.01$ and BER $= 6.16\%$. (*c*) De-noise image using a low-pass spacial filter, the output BER $= 7.67\%$. (*d*) De-noise image, first by using 2D PSR and then a low-pass spacial filter, the output BER $= 3.26\%$.

(*a*) (*b*) (*c*)

Figure 6. (*a*) Image corrupted by geometry noise with the parameter $p = 0.1$; (*b*) de-noise image using equation (20) with $\gamma = 0.35, a = -0.14, b = 0.002$ and BER $= 10.71\%$; (*c*) de-noise image using low-pass spacial filter, the output BER $= 13.49\%$. We can see many ripples and distortions due to a non-Gauss factor.

the bit error rate (BER) of the output image against the input noise intensity. From figure 2 we can see that the output BER reaches a minimum, which shows that traditional SR does exist in our image processing.

Figure 3 shows an original binary image (*a*) corrupted by the 0,0,0 additive Gaussian white noise which has intensity $D = 1$ (*b*). We first sample the corrupted image 100 times per pixel (ten by row and ten by column). Then we can optimize the system parameters γ, a, b according to the principle (19). Finally, we use equation (20) to process the noisy image. The output is shown in figure 3(*c*), as compared with the use of a traditional linear filter shown in figure 3(*d*). We can see that 2D-PSR image processing preserves more detailed characteristics (more detailed characteristics of the hair, hat, lips, etc are remained in figure 3(*c*) than in figure 3(*d*)), and the output BER is lower.

Now we increase D to 4, the outputs of 2D PSR and traditional linear filtering are shown in figure 4. Obviously, when noise intensity becomes larger, 2D PSR performs much better than low-pass filtering. That is because the 2D bistable system is robust to noise change. From the above examples, we can see that the noisy image processed by 2D PSR holds much more detailed characteristics than by linear filtering, and its output BER is lower.

Next, if we process the noisy image with a combined use of the two methods, the output will perform even better, which can be seen in figure 5. As a consequence, we can claim that the methods of 2D PSR and linear filtering are complementary.

When additive noise is not Gaussian, 2D PSR can still perform well due to its robustness, while linear filtering may perform poor, for it is more relying on noise type. This point will be transparent in the following example. To this end, let us add geometric noise [29] (parameter $p = 0.1$) with zero mean to the original image. The performances of 2D PSR and low-pass filtering are shown in figure 6. We can see that the output image, figure 6(*c*), is highly distorted due to a non-Gauss factor, while the output image, figure 6(*b*), still looks fine relatively.

4. Conclusions

This paper develops an elementary theory of two-dimensional PSR, and preliminarily reveals the potential application of SR techniques in nonlinear image processing. A novel nonlinear SR system is proposed by extending the concept of PSR from the one-dimensional case to the two-dimensional case. The stationary solution and the lower bound of the response speed of

the SR system are derived. Optimization of system parameters based on the principle (19) can minimize the bit error rate of the output image. Theoretically, calculated BER is in accordance with our simulation results.

The superiority of 2D-PSR image processing, according to the above examples, is listed below:

1. The 2D-PSR method can achieve lower BER, while holding more detailed characteristics than a low-pass filter, especially when noise intensity is large.

2. Because 2D PSR and traditional linear filters are complementary, output can be evidently improved by combining these two methods.

3. When additive noise is non-Gauss, 2D PSR, due to its robustness, will perform much better than linear filters.

Nevertheless, further research is needed to improve this method and to extend it to more complicated applications. Our findings along this line will be reported elsewhere.

Acknowledgments

This work has been supported in part by the National Natural Science Foundation of China (no 10772161) and in part by AFOSR.

References

[1] Gammaitoni L, Hanggi P, Jung P and Marchesoni F 1998 *Rev. Mod. Phys.* **70** 223–87
[2] Benzi R, Sutera A and Vulpiani A 1981 *J. Phys. A: Math. Gen.* **14** 453
[3] Harry J D, Niemi J B, Priplata A A and Collins J J 2005 *IEEE Spectr.* **42** 36–41
[4] Morse R P and Evans E F 1996 *Nature Med.* **2** 928–32
[5] Zozor S and Amblard P O 2002 *Signal Process.* **82** 353–67
[6] Stocks N G 2001 *Phys. Rev.* E **63** 041114
[7] Chapeau-Blondeau F and Rousseau D 2004 *IEEE Trans. Signal Process.* **52** 1327–34
[8] Jung P 1995 *Phys. Lett.* A **207** 93–104
[9] Inchiosa M E and Bulsara A R 1996 *Phys. Rev.* E **53** 2021–4
[10] Galdi V, Pierro V and Pinto I M 1998 *Phys. Rev.* E **57** 6470–9
[11] Kay S 2000 *IEEE Signal Process. Lett.* **7** 8–10
[12] Zozor S and Amblard P O 2003 *IEEE Trans. Signal Process.* **51** 3177–81
[13] Bulsara A R, Seberino C, Gammaitoni L, Karlsson M F, Lundqvist B and Robinson J W C 2002 *Phys. Rev.* E **67** 016120
[14] Chapeau-Blondeau F and Godvier X 1996 *Int. J. Bifurcation Chaso* **6** 2069–76
[15] Xu B, Duan F and Chapeau-Blondeau F 2004 *Phys. Rev.* E **69** 061110
[16] Xu B, Duan F, Bao R and Li J 2002 *Chaos Solitons Fractals* **13** 633–44
[17] Xu B, Li J and Zheng J 2003 *J. Phys. A: Math. Gen.* **36** 11969–80
[18] Xu B, Li J and Zheng J 2004 *Physica* A **343** 156–66
[19] Duan F and Xu B 2003 *Int. J. Bifurcation Chaos* **13** 411–25
[20] Wu X, Jiang Z and Repperger D W 2006 *American Control Conf.* pp 3118–23
[21] Wu X, Jiang Z, Repperger D W and Guo Y 2006 *CIS* **6** 1–18
[22] Chapeau-Blondeau F 2000 *Lecture Notes in Physics* vol 550 (Berlin: Springer) pp 137–55
[23] Ye Q, Huang H, He X and Zhang C 2003 *ICIP* vol 1 pp 849–52
[24] Janpaiboon S and Mitaim S 2006 *IJCNN 06* pp 2508–15
[25] Ye Q, Huang H and Zhang C 2004 *ICIP 04* vol 1 pp 263–6
[26] Risken H 1989 *The Fokker–Planck Equation: Method of Solutions and Applications (Springer Series in Synergetics* vol 18*)* 2nd edn (Berlin: Springer)
[27] Nocedal J and Wright S J 1999 *Numerical Optimization* (New York: Springer)
[28] Forsythe G E and Wasow W R 2004 *Finite-Dierence Methods for Partial Dierential Equations* (New York: Dover)
[29] Shumilov Y P, Bakut P A and Ershova O M 2002 Analysis of inner geometric noise influence on image quality of large-aperture segmented adaptive telescopes *Proc. SPIE* **4538** 162